

## Chapter 3

# Candidates and Age of the Family of Kuiper Belt Object 2003 EL61

This chapter has been published in its entirety under the same title by authors D. Ragozzine and M. E. Brown in the *Astronomical Journal*, 2007, Volume 134, pp. 2160-2167. Reproduced by permission of the American Astronomical Society. Since publication, 2003 EL61 has been renamed Haumea.

# Abstract

The collisional family of Kuiper belt object (KBO) 2003 EL61 opens the possibility for many interesting new studies of processes important in the formation and evolution of the outer solar system. As the first family in the Kuiper belt, it can be studied using techniques developed for studying asteroid families, although some modifications are necessary. Applying these modified techniques allows for a dynamical study of the 2003 EL61 family. The velocity required to change orbits is used to quantitatively identify objects near the collision. A method for identifying family members that have potentially diffused in resonances (like 2003 EL61) is also developed. Known family members are among the very closest KBOs to the collision and two new likely family members are identified: 2003 UZ117 and 1999 OY3. We also give tables of candidate family members which require future observations to confirm membership. We estimate that a minimum of  $\sim 1$  GYr is needed for resonance diffusion to produce the current position of 2003 EL61, implying that the family is likely primordial. Future refinement of the age estimate is possible once (many) more resonant objects are identified. The ancient nature of the collision contrasts with the seemingly fresh surfaces of known family members, suggesting that our understanding of outer solar system surfaces is incomplete.

## 3.1 Introduction

The collisional history of Kuiper belt objects (KBO) strongly constrains the formation and evolution of the Kuiper belt. The recent discovery by Brown et al. (2007b, hereafter B07), of a KBO family created by a collision promises new and valuable information about the early outer solar system. As the first bona fide collisional family in the Kuiper belt, it merits further study and comparison to the Hirayama collisional families in the asteroid belt. The goal of this work is to identify potential fragments for future observations and study by properly adapting techniques used in dynamical studies of asteroid families. The distribution of family members is then be used to estimate the age of the family.

Members of the 2003 EL61 family are identified by infrared spectra with strong water ice absorptions (B07), as seen in large KBO (136108) 2003 EL61 and its brightest moon (Barkume et al., 2006; Trujillo et al., 2007). Based on light curve observations, 2003 EL61 appears to be rapidly rotating with an inferred density of at least  $2.6 \text{ g cm}^{-3}$  (Rabinowitz et al., 2006), suggesting that a giant impact stripped roughly 20% of the icy mantle from the proto-2003 EL61, based on an assumed initial density of about  $2 \text{ g cm}^{-3}$  as measured for other large KBOs (e.g., Pluto, Triton). The identification of the 2003 EL61 collisional family by B07 is presumably the discovery of icy mantle fragments ejected from this giant impact. The probability of such a giant impact in the current Kuiper belt is extremely low, implying that the collision probably occurred in the early history of the outer solar system before any significant depletion in mass, as we discuss below (Morbidelli et al., 2007).

## 3.2 Dynamics

### 3.2.1 Differences between KBO and Asteroid Families

The spread in orbital elements created by a collision in the Kuiper belt is different than the previously studied asteroid belt. In both cases, a collision powerful enough to create a family launches fragments at velocities high enough to be gravitationally ejected. The ejection velocity,  $\Delta v$ , is the velocity at infinity of unbound fragments and typically scales with the escape velocity from the surface of the target. Since known KBOs (especially 2003 EL61) are much larger than typical asteroids, the expected  $\Delta v$  of a family-forming collision is much larger in the Kuiper belt. In addition, the typical orbital velocities ( $v_{orb}$ ) in the Kuiper belt are  $\sim 5 \text{ km s}^{-1}$ , compared to  $\sim 20 \text{ km s}^{-1}$  typical of the asteroid belt. The ratio of  $\Delta v/v_{orb}$  roughly determines the size of the spread in orbital elements that will be achieved by collisional dispersion. Hence, asteroid families will (initially) be far more tightly clustered in proper orbital element space than Kuiper belt families. Figure 1 shows the cloud of orbital elements created from a velocity dispersion of only  $150 \text{ m s}^{-1}$  from a potential origin of the 2003 EL61-forming collision (described in more detail below).

Asteroid families are often identified by looking only at clusters in proper orbital elements. This fails to identify true families in the Kuiper belt since the large anticipated spread in orbital elements is typically larger than the natural separation between objects (Chiang et al., 2003). The 2003 EL61 family was only identified because family members shared a unique spectral signature, in addition to being dynamically clustered. (B07)

Due to interactions with resonances, the dynamical clustering of collisional families grows weaker with time. In the asteroid belt, proper element dispersion is aided by drifting semi-major axes due to the Yarkovsky effect acting on small bodies (Farinella & Vokrouhlicky, 1999). In the Kuiper belt, objects are generally very stable over the age of the solar system except near mean-motion resonances with Neptune and/or when perihelia drop below about 35 AU (Kuchner et al., 2002).

### 3.2.2 Determining $\Delta v$

To identify dynamically-nearby KBOs for further investigation, we use  $\Delta v$  (the required ejection velocity) as a quantitative measurement of dynamical proximity. After a collision, each (unbound) fragment assumes a different heliocentric orbit, all of which intersect at the location of the collision  $(x_c, y_c, z_c)$ . At this location, each family member has a different velocity,  $\mathbf{v}_c$ . By definition,  $\Delta v$  is the length of  $(\mathbf{v}_c - \mathbf{v}_{c,cm})$ , where  $\mathbf{v}_{c,cm}$  is the velocity at the collision location of the center of mass orbit; all values of  $\Delta v$  are measured with respect to the center of mass orbit. After the collision the center of mass orbit is nearly the orbit of the largest fragment; we approximate the center of mass orbit with the post-impact orbit of 2003 EL61. Finding  $\Delta v$  would be trivial if we knew the full set of orbital elements  $(a, e, i, \Omega, \omega, M)$  for each object and 2003 EL61 at the time of the collision. Unfortunately, after a relatively short time, the coherence of the original orbital angles is lost and at the present epoch only the proper semi-major axes, proper eccentricities, and proper inclinations are known.

Even so, it is possible to use the distribution of proper elements of family members to estimate the orbital angles of the center of mass orbit (see below). Once these orbital elements are fully proscribed, there is enough information to calculate  $\Delta v$  using the additional constraint that all orbits pass through the collision location. For asteroid families, Gauss' equations are then used to compute the components of  $\Delta v$  (e.g., Morbidelli et al., 1995). These equations are only accurate if  $\Delta v \ll v$  for each component of  $v$ , whereas for the 2003 EL61 family, which has a large velocity dispersion ( $\gtrsim 200 \text{ m s}^{-1}$ ) and a relatively small orbital velocity ( $\sim 4500 \text{ m s}^{-1}$ ), Gauss' equations can lead to inaccuracies which can be avoided through a more direct calculation.

Instead, we convert the center of mass orbital elements to Cartesian coordinates, giving the collision location  $(x_c, y_c, z_c)$  and velocity  $\mathbf{v}_{c,cm}$ . We then use a direct mathematical conversion of the KBO proper elements  $(a_P, e_P, i_P)$  and the collision location  $(x_c, y_c, z_c)$  to find the orbital velocity  $\mathbf{v}_c$ . However, these six variables do not uniquely determine the velocity; there are four

possible solutions to this inversion. (This degeneracy results from two different occurrences where either the positive or negative square root can be used.) That is, a single location  $(x_c, y_c, z_c)$  can be identified by identical orbital elements  $a_P$ ,  $e_P$ , and  $i_P$  and four sets of velocities, as there is no way to distinguish between reflections along the line of apsides or the line of nodes. There is no *a priori* way to resolve this degeneracy since the information about the original orbital angles  $(\Omega, \omega, M)$  is lost. Since the goal of this study is to identify all KBOs that could potentially be members of the 2003 EL61 family, we take the smallest value of  $\Delta v$ . In this way, all KBOs with proper orbital elements that could be dynamically near the collision are identified.

To determine  $\Delta v$  of candidate family members requires the orbital elements of the center of mass orbit. This orbit is usually taken from the proper orbital elements of the largest fragment with orbital angles chosen to match the distribution of family members in  $a_P$ - $e_P$ - $i_P$  space (see Figures 1 and 2). The longitude of the ascending node ( $\Omega_{cm}$ ) has no effect on this distribution and is ignored. We use the orientation of the collisional cloud in  $a_P$  vs.  $e_P$  to find the mean anomaly ( $M_{cm}$ ); the argument of perihelion ( $\omega_{cm}$ ) has no effect here. However,  $\omega_{cm}$  does change the extent of the inclinations attainable with a particular value of  $\Delta v$ . In particular, for collisions that occur on the ecliptic ( $\omega_{cm} + M_{cm} \simeq 0^\circ$  or  $180^\circ$ ), require the lowest  $\Delta v$  to change the inclination. At the highest and lowest points of the orbit it is very difficult for a collision to change the inclination (apparent from the form of Gauss' equation for inclination changes, see Morbidelli et al. (1995)). There is not enough information in the distribution of proper elements of the family members to uniquely determine the component of  $\Delta v$  out of the plane of the orbit. In order to proceed, we choose to work with the minimum possible  $\Delta v$ , which we will call  $\Delta v_{min}$ . (The analysis in B07 did not appreciate this aspect of collisional orbit changes and assumed that  $\Delta v_{min}$  was the actual escape velocity of the fragments, which may not be true.) The component of  $\Delta v$  out of the plane of the orbit is larger by a factor of  $\sim 2$  on average (i.e., with a randomly chosen  $\omega_{cm}$ ) and at extreme points in the orbit the actual ejection velocity could theoretically be  $\sim 5$  or more times greater than  $\Delta v_{min}$ . However, collisions are most probable near the ecliptic (where the number density is highest), so the correction is probably much smaller. Furthermore, if an isotropic ejection of fragments is assumed, then this ambiguity is removed and the  $a_P$ - $e_P$ - $i_P$  distribution is sufficient to determine the typical ejection velocity (Nesvorný et al., 2006). The only way the actual ejection velocities of all the family members could have been significantly greater than  $\sim 150 \text{ m s}^{-1}$  is if they all left in a collimated jet in a particular direction from a non-ecliptic collision. Finally, we note that a similar correction factor will apply to most KBOs, roughly preserving the overall ranking of KBOs by dynamical proximity to the collision.

### 3.3 Potential Family Members

#### 3.3.1 Collision Center

For the 2003 EL61 family, we determined the center of mass orbit based on the orbit of 2003 EL61, the largest fragment. However, 2003 EL61 has diffused from its original location due to interaction in the 12:7 mean-motion resonance with Neptune (B07) and its proper elements have changed. Over long timescales, overlapping sub-resonances can cause diffusion of proper eccentricity and inclination (Nesvorný & Roig, 2001; Murray & Holman, 1997). For KBOs starting with orbital elements near the center of the 2003 EL61 family, we have found empirically that the chaotic diffusion nearly conserves the proper Tisserand parameter with respect to Neptune, the 50 MYr average of the osculating Tisserand parameter:

$$T = \frac{a_N}{a} + 2 \cos(i - i_N) \sqrt{(a/a_N)(1 - e^2)} \quad (3.1)$$

where  $a_N$  and  $i_N$  are the osculating semi-major axis and inclination of Neptune. In particular, we can estimate possible past locations of 2003 EL61 by changing the eccentricity and inclination to preserve the proper Tisserand parameter of 2003 EL61 ( $a_p=43.10$  AU and  $T_p=2.83$ ).

The pre-diffusion orbit of 2003 EL61 is estimated by minimizing the sum of  $\Delta v_{min}$  for previously identified family members (1995 SM55, 1996 TO66, 2002 TX300, 2003 OP32, and 2005 RR43) while fixing  $a_P = a_{P,EL61}$  and  $T_P = T_{P,EL61}$  and allowing the other orbital elements to vary. This results in a nominal collision location at  $(a, e, i, \omega, M)_{cm} = (43.10 \text{ AU}, 0.118, 28.2^\circ, 270.8^\circ, 75.7^\circ)$  which is used to generate Figure 1 and the values of  $\Delta v_{min}$  for family members listed in Table 3.1. (As expected, the minimal velocities are attained for values of  $\omega_{cm}$  that place the collision near the ecliptic.) The results that follow are not strongly dependent on this particular choice of the center of mass orbit. Exploring other center of mass orbits (such as the average of proper elements of non-resonant family members) indicates that the exact values of the ejection velocity vary somewhat, especially for objects near ( $\Delta v \lesssim 100 \text{ m s}^{-1}$ ) the collision, but the known family members are always tightly clustered dynamically. Figure 1 shows the extent of proper element space covered by a collision with  $\Delta v_{min}=150 \text{ m s}^{-1}$ ; this collisional cloud contains all the known family members (allowing for resonance diffusion).

#### 3.3.2 Non-resonant KBOs

Keeping in mind the large spread in osculating elements of KBOs that could belong to the 2003 EL61 family, 131 high-inclination KBOs observed over at least two oppositions were chosen for further study. These objects were integrated using the n-body code SyMBA (Levison & Duncan, 1994) using the integrator `swift_rmvs3` based on the mapping by Wisdom & Holman (1991). The integration

proceeded backwards in time with 40-day timesteps from epoch JD 2451545.0 and included the 4 outer planets and the KBOs as test particles with initial conditions given by JPL HORIZONS<sup>1</sup>. Proper elements were taken as the 50 MYr average of the corresponding osculating elements.

Using the center of mass orbit found above reveals that 2003 UZ117 and 2005 CB79 have small values of  $\Delta v_{min}$ , less than some known fragments. (No other KBOs have significantly smaller  $\Delta v_{min}$  than known family members.) KBO 2003 UZ117 has unpublished colors obtained by Tegler et al.<sup>2</sup> that show it has a clearly neutral color gradient. As shown in B07, all family members have blue/neutral visible color gradients (see Table 3.1 and references therein). Although future infrared observations are necessary, since this object has a strongly consistent color and is dynamically within the core of other known fragments, we will consider it a member of the 2003 EL61 family. No color or spectral information is available for 2005 CB79, but it has a very low  $\Delta v_{min}$  and is an excellent candidate family member.

We now seek a meaningful self-consistent value of  $\Delta v_{min}$  for other KBOs which may or may not be other family members. Allowing the center of mass orbital angles to vary can significantly change the shape of the collisional cloud and the values of  $\Delta v$  as illustrated in Figure 3.2. We could use the center of mass orbit found above (thin lines in Figure 3.2), but the small number of family members and their tight clustering does not provide a unique constraint for the orbital angles. On the other hand, the orbital angles that minimize  $\Delta v$  for each individual KBO may result in a collisional cloud that is inconsistent with the distribution of known family members (dotted line in Figure 3.2). As a compromise, we define  $\Delta v_{min}$  for candidate KBOs as the minimum  $\Delta v$  found by varying the orbital angles under the constraint that all known family members must lie within the resulting collisional cloud (thick solid curve in Figure 3.2). In other words, the angles are allowed to vary so long as the candidate KBO has larger  $\Delta v_{min}$  than all the known family members. This compromise allows for flexibility in estimating the center of mass orbital angles that are compatible with the known family members.

The results of this analysis are given in Table 3.1. For those KBOs known to be family members, accounting for errors in the orbital elements (as listed on the AstDys website<sup>3</sup>) caused variations in  $\Delta v_{min}$  of less than 5-10%.

---

<sup>1</sup><http://ssd.jpl.nasa.gov/horizons.cgi>

<sup>2</sup><http://www.physics.nau.edu/~tegeler/research/survey.htm>

<sup>3</sup><http://hamilton.dm.unipi.it/cgi-bin/astdys/astibo>

Table 3.1. KBOs Near the 2003 EL61 Family

Name	$\Delta v_{min}$	$a_P$ (AU)	$e_P$	$i_P$ ( $^\circ$ )	$T_P$	$H^a$	Visible Gradient <sup>b</sup>	Comments on Infrared Spectra	References
1996 TO66	24.2	43.32	0.12	28.02	2.83	4.50	$2.38 \pm 2.04$	Strong Water Ice	3,5
2003 UZ117	66.8	44.26	0.13	27.88	2.84	5.20	$0.00 \pm 1.96$	(Strong Water Ice)?	6
2005 CB79	96.7	43.27	0.13	27.17	2.84	5.0	NA		
2002 TX300	107.5	43.29	0.13	26.98	2.84	3.09	$0.00 \pm 0.67$	Strong Water Ice	3
2005 RR43	111.2	43.27	0.13	27.07	2.84	4.00	NA	Strong Water Ice	3
2003 OP32	123.3	43.24	0.10	27.05	2.85	4.10	$-1.09 \pm 2.20$	Strong Water Ice	3
2005 FY9	141.2	45.56	0.16	27.63	2.84	-0.23	NA	Methane Ice	1
2002 GH32	141.9	42.04	0.09	27.59	2.83	5.50	$35.25 \pm 10.21$		4
1998 HL151	142.5	40.80	0.09	27.82	2.82	8.10	$9.83 \pm 21.2$		4
2003 SQ317	148.0	42.67	0.09	28.16	2.83	6.30	NA		
1995 SM55	149.7	41.84	0.10	26.85	2.84	4.80	$1.79 \pm 2.60$	Strong Water Ice	3,5
1999 OK4	161.5	43.30	0.15	28.58	2.81	7.60	NA		
2004 PT107	198.3	40.60	0.06	27.32	2.83	5.60	NA		
2005 UQ513	199.2	43.46	0.16	27.12	2.84	3.7	NA	Weak Water Ice	2
2003 HA57	214.3	39.44	0.15	28.40	2.78	8.10	NA		
2004 SB60	221.0	42.08	0.10	25.59	2.86	4.40	NA		
2003 TH58	229.6	39.44	0.06	29.50	2.78	7.60	NA		
1998 WT31	233.3	46.04	0.19	27.91	2.83	7.05	$5.57 \pm 5.61$		4
2002 AW197	265.0	47.28	0.12	26.00	2.90	3.27	$22.45 \pm 1.62$	No Water Ice	3
1996 RQ20	269.9	43.89	0.10	31.74	2.76	6.95	$19.81 \pm 6.31$	IR Colors Inconsistent	4,5
1999 OY3	292.8	43.92	0.17	25.80	2.86	6.76	$-2.62 \pm 3.39$	Vis and IR Colors of Strong Water Ice	4,5
1999 OH4	305.1	40.52	0.04	26.71	2.84	8.30	NA	IR Colors Inconsistent	5
1997 RX9	306.1	41.62	0.05	29.31	2.80	8.30	NA		
2001 QC298	310.2	46.32	0.13	31.59	2.78	6.09	NA	IR Colors Inconsistent	5
2003 EL61 <sup>c</sup>	323.5	43.10	0.19	26.85	2.83	0.27	$-0.18 \pm 0.67$	Strong Water Ice	3
2000 CG105	330.6	46.38	0.04	29.43	2.84	6.50	$2.58 \pm 17.72$	IR Colors Inconsistent	4,5
2003 HX56	363.2	47.32	0.21	30.00	2.79	7.10	NA		
1999 CD158	364.0	43.71	0.15	23.83	2.90	5.05	$16.36 \pm 3.41$	IR Colors Inconsistent	4,5

References. — (1) Brown et al. (2007a) (2) Barkume et al. in press (3) Brown et al. (2007) (4) MBOSS Database <http://www.sc.eso.org/~chainaut/MBOSS/> and references therein (5) Noll et al. (2005) (6) Tegler et al. website <http://www.physics.nau.edu/teglert/research/survey.htm>

Note. — As explained in the text,  $\Delta v_{min}$  is the minimum ejection velocity required to reach the orbit of the listed KBO from the modeled 2003 EL61 family-forming collision in  $\text{m s}^{-1}$ . The actual ejection velocities could be different, but the relative order should be roughly correct. Known family members have visible color gradients near zero and strong water ice spectra. Other objects listed could be family members or interlopers.

<sup>a</sup>Absolute Magnitude

<sup>b</sup>As defined in References 1 and 4. Objects without published colors list "NA".

<sup>c</sup>This refers to the current proper elements, without allowing diffusion.



The blue/neutral visible color gradients of 1998 HL151 and 1998 WT31 are similar to known family members (see Tables 3.1 and 3.2 and references therein). Blue colors are suggestive, but do not necessarily imply the strong water ice spectrum that characterizes this family (B07). Without observational evidence of a water-ice spectrum, we cannot confirm whether these objects are 2003 EL61 family members or merely interlopers, which appears to be the case for 2002 GH32 and others which have red visible color gradients. Table(s) 3.1 (and 3.2) then serves as a guide for future observations.

### 3.3.3 Resonant KBOs

As a consequence of the wide dispersion of fragments from a collision in the Kuiper belt, many objects can be injected into various mean-motion resonances with Neptune. While KBOs in low-order resonances (e.g., 3:2) can be stable for the age of the solar system, objects in high-order resonances (found throughout the region of the 2003 EL61 family) will experience chaotic diffusion, as discussed above. Over timescales of tens of millions to billions of years, the proper eccentricity and inclination of resonant KBOs are not conserved. These objects can not be directly connected to the family based on current proper elements because their proper elements have changed since the formation of the family. How then can we identify such fragments? In the case of 2003 EL61, it is the consistent strong water ice spectrum, as well as several indications of a past giant impact, that connect it to the non-resonant objects. Similarly, in the asteroid belt, the Eos family intersects the 4:9 Jovian resonance and objects in the resonance have diffused in eccentricity and inclination (Morbidelli et al., 1995). Spectroscopic studies of a few asteroids in the resonance showed them to be uniquely identifiable and consistent with the rest of the Eos family, confirming that these fugitives are collisionally linked (Zappalà et al., 2000).

For resonant KBOs that have not yet diffused to scattered or low-perihelion orbits, the Tisserand parameter with respect to Neptune,  $T$ , can be used as a reasonable dynamical criterion for family membership. Through forward modeling, we have verified that the velocity dispersion ( $\Delta v \lesssim 300 \text{ m s}^{-1}$ ) due to the collision and the forced variation of osculating elements in time together cause maximal variations in  $T$  of about  $\sim 0.1$  from  $\sim 2.85$ . Only about 16% of multi-opposition KBOs have a Tisserand parameter between 2.74 and 2.96, and these were included in our integrations of KBOs.

To identify candidate fragments that could have diffused in resonances, we allowed the proper eccentricity and inclination of each KBO to vary, conserving the proper Tisserand parameter, while the semi-major axis of the KBO was fixed to  $a_P$ . The minimal velocity distance, found using the method described above, is called  $\delta v_{min}$  to distinguish it from the velocity computed with the current proper elements and is listed in Table 3.2. Of course, this value of  $\delta v_{min}$  will always be less than the corresponding  $\Delta v_{min}$  computed with unadjustable proper elements and will increase the

number of interlopers. Even so, it can give an indication of objects that had low ejection velocities and subsequently diffused in a resonance. Table 3.2 lists the resonances present in our integration of these objects. Even for multi-opposition KBOs, current membership in any of the many weak resonances in this region can be easily obscured within the errors in the determination of orbital elements. To be conservative, we calculate  $\delta v_{min}$  for all KBOs in our integration. A lack of resonance identification in Table 3.2 is not meant to imply that these objects have not actually been affected by proper element diffusion.

Table 3.2. Diffused KBOs Near the 2003 EL61 Family

Name	$\delta v_{min}$	$a_P$ (AU)	$e_{min}$	$i_{min}$ ( $^{\circ}$ )	$T_P$	$H^a$	Visible Gradient <sup>b</sup>	Comments on Infrared Spectra	Resonance	References
1996 TO66	15.0	43.32	0.11	28.09	2.83	4.50	$2.38 \pm 2.04$	Strong Water Ice	19:11	3,5
2003 SQ317	31.4	42.67	0.11	27.92	2.83	6.30	NA			
2005 UQ513	39.0	43.27	0.12	27.77	2.84	5.0	NA	Weak Water Ice		2
2005 RR43	58.0	43.27	0.11	27.38	2.84	4.00	NA	Strong Water Ice		3
2003 UZ117	60.8	44.26	0.12	28.01	2.84	5.20	$0.00 \pm 1.96$	(Strong Water Ice)?		6
2005 CB79	66.5	43.27	0.11	27.40	2.84	5.0	NA			
2002 TX300	68.4	43.29	0.11	27.23	2.84	3.09	$0.00 \pm 0.67$	Strong Water Ice		3
1999 OK4	72.5	43.30	0.12	29.16	2.81	7.60	NA			
2002 GH32	79.3	42.04	0.10	27.50	2.83	5.50	$35.25 \pm 10.21$			4
1997 RX9	86.8	41.62	0.13	28.46	2.80	8.30	NA			
2003 OP32	91.4	43.24	0.11	26.90	2.85	4.10	$-1.09 \pm 2.20$	Strong Water Ice		3
1999 OY3	96.6	43.92	0.10	27.00	2.86	6.76	$-2.62 \pm 3.39$	IR Colors of Strong Water Ice	<sup>c</sup>	4,5
2005 FY9	118.0	45.56	0.15	27.87	2.84	-0.23	NA	Methane Ice		1
1995 SM55	123.3	41.84	0.09	26.98	2.84	4.80	$1.79 \pm 2.60$	Strong Water Ice		3,5
1998 HL151	136.4	40.80	0.11	27.55	2.82	8.10	$9.83 \pm 21.2$			4
1998 WT31	139.8	46.04	0.16	28.57	2.83	7.05	$5.57 \pm 5.61$			4
2000 CG105	149.0	46.38	0.16	28.04	2.84	6.50	$2.58 \pm 17.72$	IR Colors Inconsistent		4,5
2004 PT107	161.9	40.60	0.09	27.08	2.83	5.60	NA			
1999 RY215	183.0	45.28	0.11	26.37	2.88	6.13	$4.54 \pm 6.65$	IR Colors Inconsistent		4,5
2001 FU172	200.0	39.44	0.08	28.62	2.80	8.30	NA		3:2	
1999 OH4	200.5	40.52	0.08	26.45	2.84	8.30	NA	IR Colors Inconsistent		5
2003 HA57	212.3	39.44	0.12	28.80	2.78	8.10	NA		3:2	
2003 TH58	214.7	39.44	0.13	28.82	2.78	7.60	NA		3:2	
2004 SB60	218.5	42.08	0.10	25.63	2.86	4.40	NA			
2003 QX91	222.0	43.71	0.12	31.03	2.77	8.30	NA		7:4	
2000 JG81	235.1	47.77	0.12	27.42	2.88	9.10	NA		2:1	
1999 KR16	242.9	49.00	0.22	28.34	2.84	5.70	$44.74 \pm 3.21$	IR Colors Inconsistent		4
2005 GE187	243.5	39.44	0.07	26.50	2.84	7.10	NA		3:2	
1996 TR66	248.3	47.78	0.11	26.94	2.89	7.50	NA	IR Colors Inconsistent		5

References. — (1) Brown et al. (2007a) (2) Barkume et al. in press (3) Brown et al. (2007) (4) MBOSS Database <http://www.sc.eso.org/ohainaut/MBOSS/> and references therein (5) Noll et al. (2005) (6) Tegler et al. website <http://www.physics.nau.edu/~teglert/research/survey.htm>

Note. — As explained in the text,  $\delta v_{min}$  is the minimum ejection velocity required to reach an orbit with the same proper semi-major axis ( $a_P$ ) and proper Tisserand parameter ( $T_P$ ) of the listed KBOs in  $\text{m s}^{-1}$ . Integrations indicate  $T_P$  is nearly conserved during eccentricity and inclination diffusion in mean-motion resonances. By construction, 2003 EL61 is the center of the collision (allowing diffusion). For those objects which are resonant in our integration (identified by libration of the resonance angle in the past 4 MYr), the resonance type is listed. Many more objects may be in resonance within the errors of orbit determination (e.g., 1999 OY3), which were not accounted for here.

<sup>a</sup>Absolute Magnitude

<sup>b</sup>As defined in References 1 and 4. Objects without published colors list "NA".

<sup>c</sup>1999 OY3 is probably affected by the 7:4 resonance.

As with non-resonant objects, good spectroscopic evidence is required to consider these objects part of the 2003 EL61 family. KBO 1999 OY3 has reported near-infrared colors consistent with other family members, which have unique colors due to the presence of strong water ice absorptions (Noll et al., 2005). Integrations of clones of this KBO that include errors in orbital elements show that there is a high probability that it is in the 7:4 mean motion resonance. It also has a very low resonant  $\delta v_{min}$  and, like 2003 EL61 and 1996 TO66, appears to be a family member in a resonance. 2005 UQ513 has a very low  $\delta v_{min}$ , but does not have the characteristic spectral features of the family members.

### 3.4 Age of the Family

Determining the age of the 2003 EL61 family will allow new insights into the history of the Kuiper belt. It is possible to constrain the age because the shape of a collisional cloud will evolve in time by resonance diffusion (Milani & Farinella, 1994). In each resonance, the changing eccentricity distribution of KBOs can be computed by numerical integrations. (Throughout this section, all orbital elements refer to proper orbital elements.) As resonance diffusion is chaotic, ages cannot be calculated by back-integration of known particles. Instead, an ensemble of particles (with an assumed initial distribution of eccentricities) is integrated forward for the age of the solar system. Comparing the eccentricities of remaining particles to the eccentricities of known family members results in an age estimate.

#### 3.4.1 Diffusion Time of 2003 EL61

One estimate of the age of the family is the time needed for 2003 EL61 to diffuse from its original eccentricity to the current value. Matching the distribution of known family members above has yielded an estimate of the initial eccentricity and inclination of 2003 EL61 before diffusion, assuming that its displacement from the center of the family is small (which is expected from conservation of momentum). From an ensemble of randomly placed test particles, 78 particles in the 12:7 resonance with low values of  $\Delta v$  from the collision center (near  $e_{P,orig} = .118$ ) were chosen for long-term integration. Again using SyMBA with a 40-day timestep, these particles were integrated for the age of the solar system. The initial configurations of the planets were also randomly chosen (by randomly choosing the starting epoch in the past 100 MYr). As expected from the chaotic nature of resonance diffusion, the results do not significantly depend on the orientation of the planets or even the initial location of 2003 EL61. Initial eccentricities ranged from 0.09 to 0.14, but other than a slight preference for higher eccentricity particles to escape sooner, the calculated diffusion times were similar.

The current proper perihelion of 2003 EL61 is 35 AU, the approximate limit for stability against

close encounters with Neptune. In our simulations, particles are usually removed shortly after attaining the current eccentricity of EL61  $e_{P,now} = 0.186$ , though they occasionally diffuse back down to lower eccentricities. In Figure 3.3, we have plotted the fraction of particles with proper eccentricities below  $e_{P,now}$  as a function of time. Nearly 90% of the particles have not diffused the full distance a billion years into the integrations. After 3.5 billion years of evolution, roughly half of the particles have reached the current eccentricity of 2003 EL61. We conclude that with 90% confidence, the 2003 EL61 family is older than 1 GYr, with an age estimate of  $3.5 \pm 2$  GYr (1-sigma). Importantly, the age is completely consistent with formation at the beginning of the solar system: the family is ancient and likely primordial.

### 3.4.2 Diffusion Time of Other Resonant Family Members

As the progenitor of the collision, the resonance diffusion of 2003 EL61 is a special case because it is a unique object. For other family members, a similar analysis would require assumptions about the number of similar objects captured in each resonance. To avoid unnecessary assumptions, we propose a simple method for estimating the age of the family by using the eccentricity distribution of family members currently in the resonance instead of focusing on any single particle. The initial eccentricity distribution in a resonance can be inferred from the eccentricity distribution of nearby non-resonant particles whose (proper) eccentricities are essentially constant for the age of the solar system. Integrating an ensemble of particles with the same starting eccentricities will produce an evolving eccentricity distribution. As an example, consider the eccentricity evolution for the 12:7 resonants shown in Figure 3.4; only the eccentricities of objects still in the resonance are shown. After debiasing the eccentricity distribution of known family members for detection biases, the current eccentricity distribution can be statistically compared with the integrations. As it uses only the distribution of remaining eccentricities, this method does not require any assumptions about the efficiency of initial emplacement in or removal from the resonance in question.

The characteristic diffusion timescale of these resonances strongly depends on the order or strength of the resonance. While 2003 EL61 is in the fifth-order 12:7 resonance, 1996 TO66 appears to be in the weaker eighth-order 19:11 resonance. Over the age of the solar system, the proper eccentricities of 19:11 resonants (near the current location of TO66) only change by 0.01-0.02; this is less than the accuracy with which one could infer the unknown initial location of these objects. The eccentricity distribution of objects in such weak resonances are essentially constant in time and therefore cannot provide a meaningful age constraint.

In contrast, 1999 OY3 is in the strong third-order 7:4 resonance. In addition to increased diffusion times, 7:4 resonants often participate in the Kozai resonance which allows for exchange of angular momentum between eccentricity and inclination (Lykawka & Mukai, 2005). Particles near the assumed starting position of OY3 unpredictably enter and leave the Kozai resonance, potentially

causing huge swings in eccentricity (as these are all high inclination particles) on very short (MYr) timescales. Practically any current eccentricity could have possibly been generated by the Kozai resonance in less than 10 MYr. Therefore, this resonance also appears to be a fruitless source of useful age constraints from eccentricity diffusion. It is important to note here that the assumption of constant  $T_P$  is often violated by these particles; the Kozai resonance carries them to low perihelia where they interact with Neptune (which is itself interacting with the other giant planets) often causing a change in  $T_P$ . Therefore, KBOs with low perihelia in the past or present are susceptible to inaccurate estimations of the initial ejection velocity ( $\delta v_{min}$ ). Although these particles can be significantly perturbed, in an integration of 20 particles in the 7:4 resonance starting near the estimated initial conditions of OY3, half are still in the resonance after 4.5 GYr.

### 3.4.3 Future Age Estimates

In the future, more family members will be identified in resonances that will, like the 12:7 resonance, have diffusion timescales that are neither too slow nor too fast. The addition of several new family members will allow for further refinement of these age estimates.

It is possible to evaluate the number of resonant particles needed to make a significant improvement upon our age estimate of  $3.5 \pm 2$  GYr. From the distributions of remaining 12:7 resonants shown in Figure 3.4, we randomly drew 5, 10, 50, and 100 eccentricities with replacement at half-billion year intervals from particles that were still in the resonance. Every pair of distributions was inter-compared using the Kuiper variant of the K-S test which returns a significance near 1 if the distributions are distinguishable statistically. This process (of random selection and cross-comparison) was repeated 100 times and the results averaged. Figure 3.5 shows some of the results of this analysis. For example, if the actual age of the family is 3.5 GYr (Figure 3.5, upper right) then with  $\sim 50$  particles (triangles), an age of 2.5 GYr or younger can be ruled out since these eccentricity distributions are different with greater than 90% significance. With  $\sim 100$  resonant particles, the accuracy in the age determination can generally be brought down to 0.5 GYr.

Unfortunately, the chaotic nature of eccentricity diffusion makes it difficult to determine a precise age without a large number of objects. However, it should be noted that each resonance gives an essentially independent measure of the age so that a total of 50-100 known family members in the appropriate (e.g., not too fast or too slow) resonances should be sufficient to get a relatively precise age estimate. In the near future, as the high-inclination region of the Kuiper belt is probed much more deeply, many new family members should be readily discovered.

### 3.5 Discussion

Identifying more 2003 EL61 family members is very useful for learning more about this family and its relationship to the formation and evolution of the outer solar system. Based on dynamical and observational evidence, we add 2003 UZ117 and 1999 OY3 to the list of 2003 EL61 family members, although the former should be observed in the infrared for confirmation of a strong water ice signature.

Due to the highly dispersive nature of large Kuiper belt collisions, some simplifications were made to identify potential family members. The computed values of  $\Delta v_{min}$  (Table 3.1) and especially  $\delta v_{min}$  (Table 3.2) could be significantly different from the true ejection velocities. Even so, we find it highly significant that all of the known fragments of the 2003 EL61 family can be explained by a velocity dispersion of  $150 \text{ m s}^{-1}$  from a single collision location, and allowing the objects in resonances to diffuse in eccentricity. In addition, all known KBOs near the proposed collision have strong water ice signatures, including the strongest such absorption features known in the Kuiper belt (except possibly 2003 UZ117, whose spectrum is unknown) (B07). Combining dynamical and spectroscopic evidence, the 2003 EL61 family currently includes, in order of decreasing absolute magnitude: (136108) 2003 EL61, (55636) 2002 TX300, (145453) 2005 RR43, (120178) 2003 OP32, (19308) 1996 TO66, (24835) 1995 SM55, 2003 UZ117, and (86047) 1999 OY3.

Many potential family members have no known photometric or spectroscopic observations. Observations of near-infrared colors on these objects will help to distinguish family members from interlopers. Discovery of additional family members will do much to improve our understanding of this family and the outer solar system. In particular, fragments in resonances have the unique ability to constrain the age of the collisional family as eccentricity diffusion, though chaotic, is time dependent. Based on the time needed for 2003 EL61 to diffuse to its current location, the family-forming collision occurred at least a billion years ago. Indeed, the probability of such a collision is only reasonable in the primordial Kuiper belt when the number densities of large KBOs was much higher. However, the collision should have occurred after any significant dynamical stirring as the orbital distribution of the family remains tight and seemingly unperturbed.

There appears to be no dynamical evidence that is not consistent with the formation of the 2003 EL61 family by an ancient collision. It is therefore interesting that all family members appear to be bright and pristine with strong crystalline water ice spectra. (B07) These surfaces seem to be exceptions to the premise that all static surfaces in the outer solar system darken and redden in time (e.g., Luu & Jewitt, 1996). This is not due to their location in the outer solar system, as there are KBOs dynamically nearby with red spectrally-featureless surfaces (see Tables 3.1 and 3.2). Perhaps the collision was energetic enough to sublimate and lose volatiles before they were able to transform into the higher-order hydrocarbons that are thought to be the darkening reddening agent

dominant in the outer solar system. However, this does not really distinguish these family members from all KBOs, at least some of which should have experienced similarly energetic impacts. Instead, the distinguishing characteristic may be that the relatively large proto-2003 EL61 was able to fully differentiate and the resulting fragments were compositionally much purer than other objects, even fragments from non-differentiated progenitors. In any case, the unique spectra of family members promise to improve our understanding of outer solar system surface processes (Barkume et al. 2007, in press).

Understanding the surfaces of KBOs is one of many insights provided by the likely primordial nature of the 2003 EL61 family. Another is the apparent need for higher number densities in the past if the family-forming collision is to be rendered probable. Continuing identification and characterization of family members can uniquely improve our understanding of this collision and its connection to the formation and evolution of the outer solar system.

*Acknowledgments:* We would like to thank Kris Barkume, Alessandro Morbidelli, Keith Noll, Emily Schaller, Meg Schwamb, and Jack Wisdom for valuable discussions. We would like to thank the referee (David Nesvorný) for timely reviews that improved the quality of this paper. DR is grateful for the support of the Moore Foundation.



# Bibliography

- Barkume, K. M., Brown, M. E., & Schaller, E. L. 2006, *Astrophysical Journal, Letters*, 640, L87.  
[astro-ph/0601534](#)
- Brown, M. E., Barkume, K. M., Blake, G. A., Schaller, E. L., Rabinowitz, D. L., Roe, H. G., & Trujillo, C. A. 2007a, *Astronomical Journal*, 133, 284
- Brown, M. E., Barkume, K. M., Ragozzine, D., & Schaller, E. L. 2007b, *Nature*, 446, 294
- Chiang, E. I., Loring, J. R., Millis, R. L., Buie, M. W., Wasserman, L. H., & Meech, K. J. 2003, *Earth Moon and Planets*, 92, 49
- Farinella, P., & Vokrouhlicky, D. 1999, *Science*, 283, 1507
- Kuchner, M. J., Brown, M. E., & Holman, M. 2002, *Astronomical Journal*, 124, 1221.  
[astro-ph/0206260](#)
- Levison, H. F., & Duncan, M. J. 1994, *Icarus*, 108, 18
- Luu, J., & Jewitt, D. 1996, *Astronomical Journal*, 112, 2310
- Lykawka, P. S., & Mukai, T. 2005, *Planetary Space Science*, 53, 1175
- Milani, A., & Farinella, P. 1994, *Nature*, 370, 40
- Morbidelli, A., Levison, H. F., & Gomes, R. 2007, *ArXiv Astrophysics e-prints*. [astro-ph/0703558](#)
- Morbidelli, A., Zappala, V., Moons, M., Cellino, A., & Gonczi, R. 1995, *Icarus*, 118, 132
- Murray, N., & Holman, M. 1997, *Astronomical Journal*, 114, 1246
- Nesvorný, D., Enke, B. L., Bottke, W. F., Durda, D. D., Asphaug, E., & Richardson, D. C. 2006, *Icarus*, 183, 296
- Nesvorný, D., & Roig, F. 2001, *Icarus*, 150, 104
- Noll, K., Stephens, D., Grundy, W., Cruikshank, D., Romanishin, W., & Tegler, S. 2005, in *Bulletin of the American Astronomical Society*, 746
- Rabinowitz, D. L., Barkume, K., Brown, M. E., Roe, H., Schwartz, M., Tourtellotte, S., & Trujillo, C. 2006, *Astrophysical Journal*, 639, 1238. [astro-ph/0509401](#)
- Trujillo, C. A., Brown, M. E., Barkume, K. M., Schaller, E. L., & Rabinowitz, D. L. 2007, *Astrophysical Journal*, 655, 1172. [astro-ph/0601618](#)
- Wisdom, J., & Holman, M. 1991, *Astronomical Journal*, 102, 1528
- Zappalà, V., Bendjoya, P., Cellino, A., Di Martino, M., Doressoundiram, A., Manara, A., & Miglior-

ini, F. 2000, *Icarus*, 145, 4

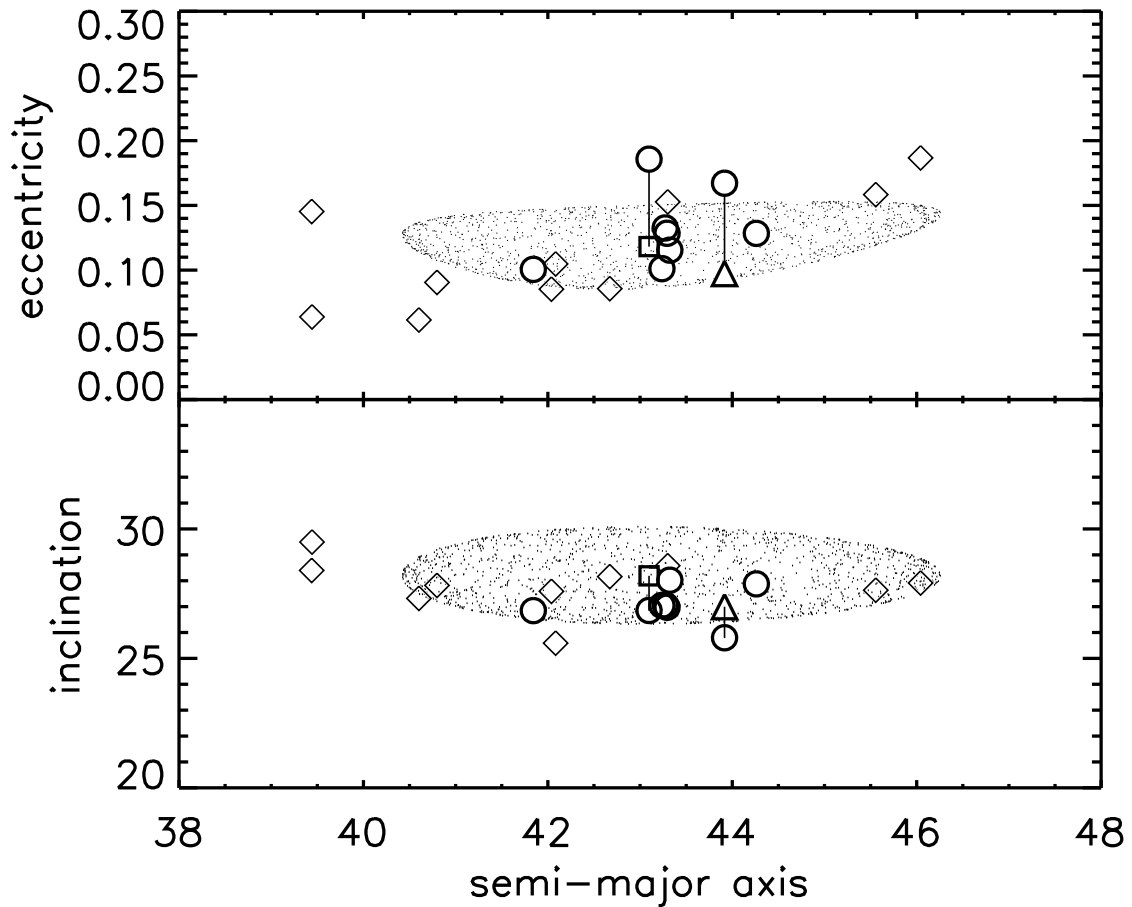


Figure 3.1 Current proper orbital elements of members of the 2003 EL61 family (circles) and potential family members (diamonds). The cloud of small points illustrate the dispersion in semi-major axis, eccentricity, and inclination of objects ejected from the nominal collision location (located at the center of the square) with an isotropic  $\Delta v$  of  $150 \text{ m s}^{-1}$ , enough to explain all the currently known members of the 2003 EL61 family. (Note that the orbital angles are chosen to minimize  $\Delta v$ ; the actual ejection velocities may be larger.) The square identifies the calculated location of the collision center which is assumed to be the initial location of 2003 EL61 before resonance diffusion (marked by vertical lines). The two rightmost circles are the current proper elements of 1999 OY3 and 2003 UZ117, new family members identified in this work. KBO 1999 OY3 (which has visible and infrared colors consistent with family members) is also allowed to diffuse to the location marked by the triangle (see Table 3.2). The proper elements of other KBOs with  $\Delta v < 250 \text{ m s}^{-1}$  (listed in Table 3.1) are shown as diamonds.

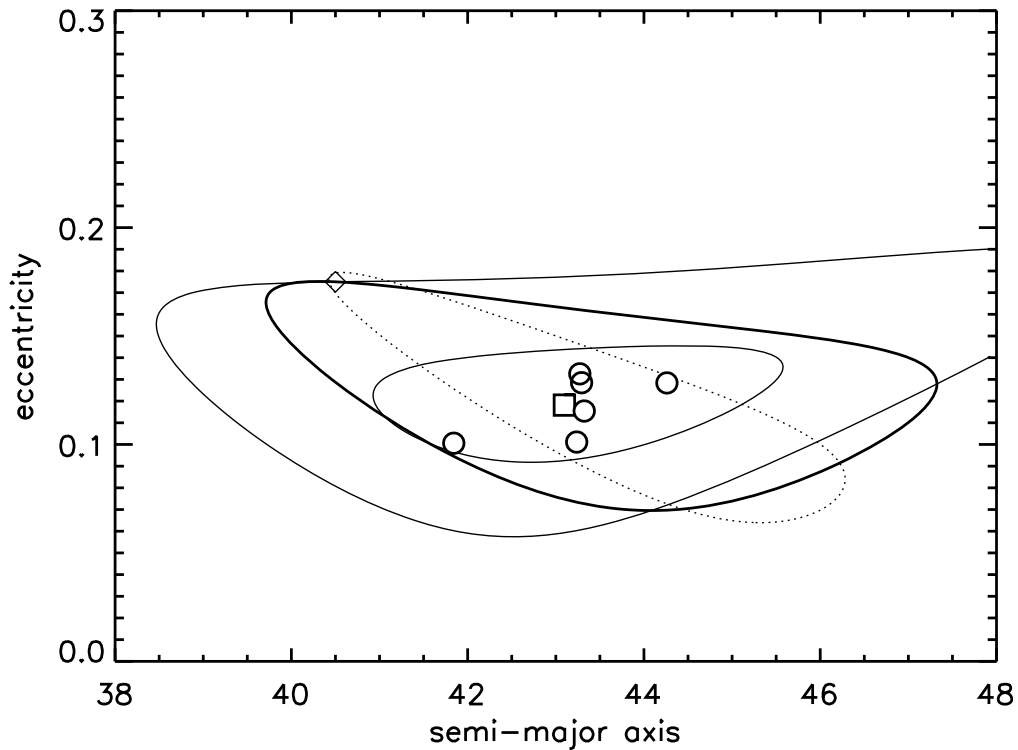


Figure 3.2 Illustration of determining  $\Delta v$  for candidate family members. The known (non-diffusing) family members (circles) fall into a relatively small region of proper orbital element space. (In this illustration, inclinations are held constant and collisions are located near the ecliptic.) These can be explained by ejection from the center of mass orbit (square) with  $\Delta v$  of  $150 \text{ m s}^{-1}$  or less, marked by the smallest thin solid curve. A hypothetical KBO (diamond) can be explained with larger  $\Delta v$  from the same center of mass orbit, shown by the larger thin curve. Alternatively, by changing the orbital angles, particularly the mean anomaly, the shape of the collisional cloud can also change requiring a much smaller  $\Delta v$  (dotted curve). However, the resulting angle may be inconsistent with the distribution of known family members, as in the case above. As a compromise between these two methods, we find the  $\Delta v_{min}$  for KBOs by allowing the center of mass orbital angles to vary with the constraint that all known family members must lie within the collisional cloud (thick solid curve).

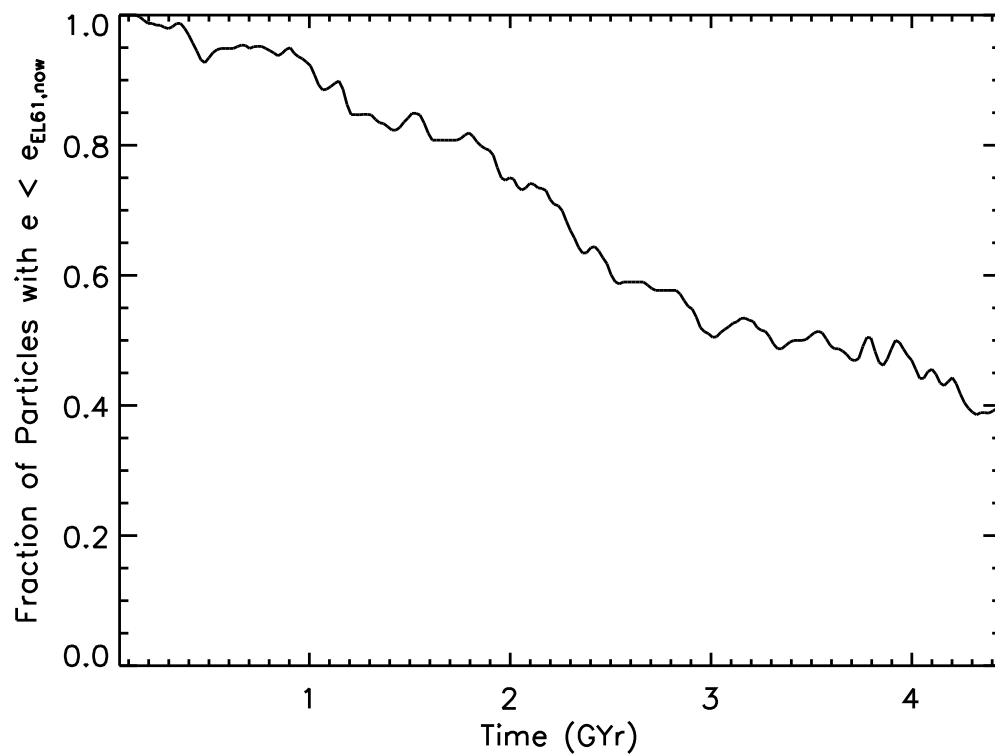


Figure 3.3 Fraction of particles that have eccentricities less than the current eccentricity of 2003 EL61 ( $e_P < 0.186$ ). Calculated from an integration of 78 12:7 resonants with initial eccentricities near 0.118 (the expected initial eccentricity of 2003 EL61). The current location of 2003 EL61 is attained by 10% of resonant KBOs in less than  $\sim 1$  GYr. After nearly 4 GYr of evolution, half the particles have passed the current location of 2003 EL61. We conclude that the 2003 EL61 family is ancient and probably primordial.

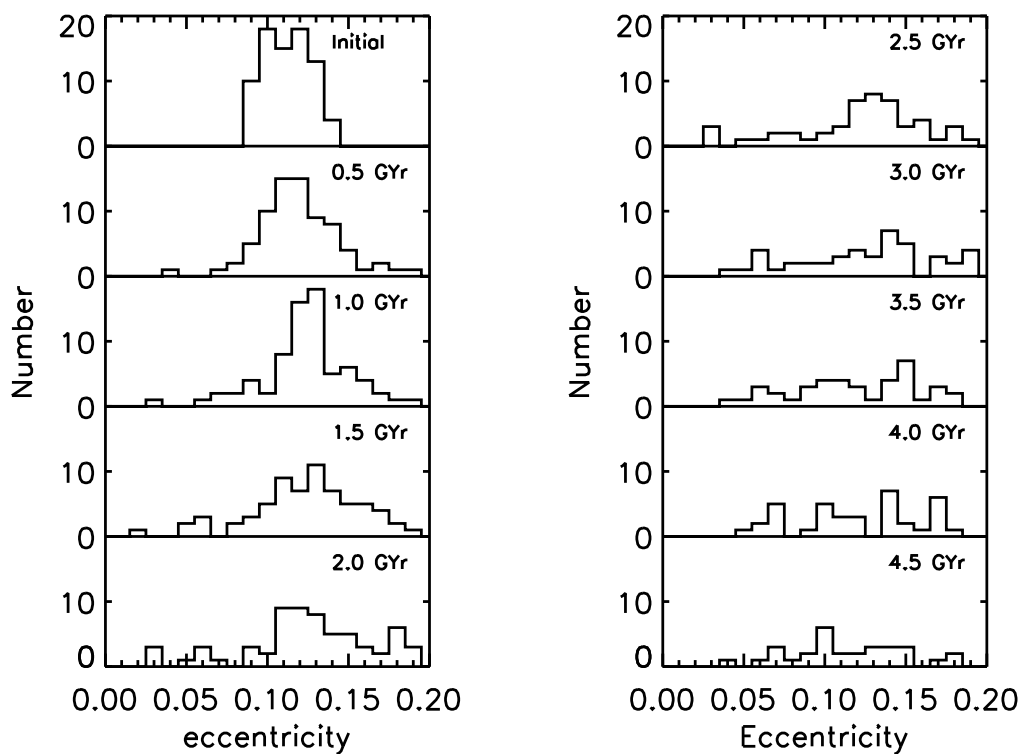


Figure 3.4 Distribution of eccentricities of 12:7 resonants at half-billion year intervals. Only particles remaining in the resonance are shown. The bin size is 0.01 in eccentricity. A clear diffusion-like spreading is evident in the widening of the initial peak. The eccentricities of KBOs in this resonance will have a distribution that can be compared to these distributions in order to estimate an age.

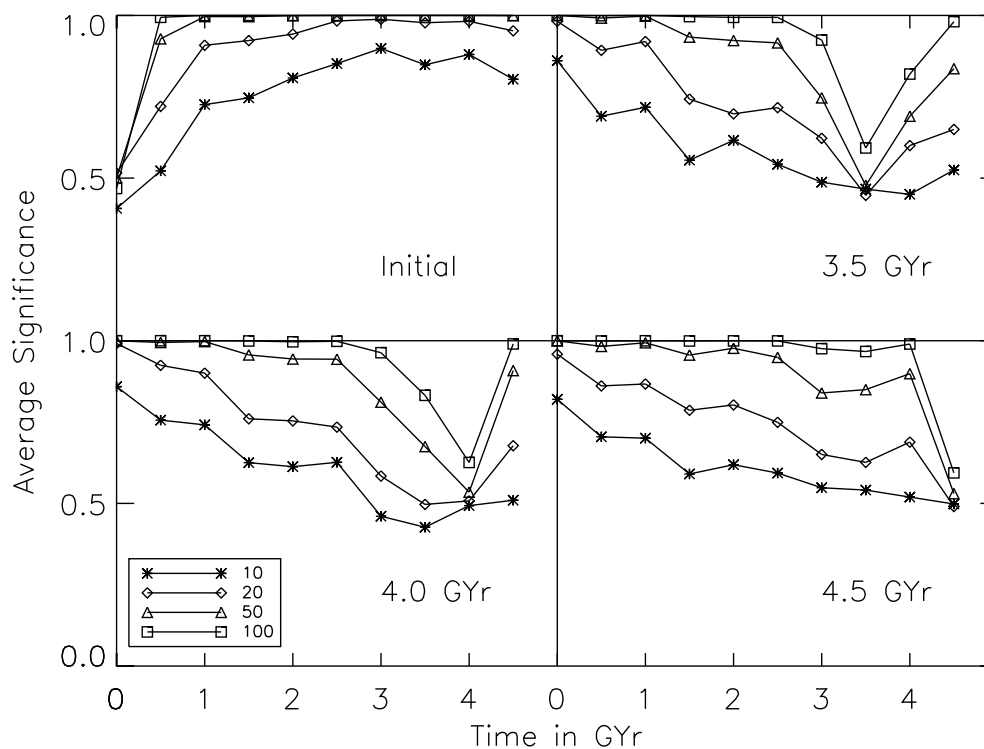


Figure 3.5 Correlations of eccentricity distributions with each other. As explained in the text, a random sample of particles is chosen from two ages and compared using the Kuiper variant of the K-S test. The probability that the two distributions are different is represented by the significance. The cross-comparisons with all ages are shown for the initial distribution (upper left) and the distributions at 3.5 GYr (upper right), 4.0 GYr (lower left), and 4.5 GYr (lower right). As expected the significance of being drawn from different populations is least when the distribution at each age is compared with itself. The different symbols represent the number of particles drawn from each distribution as shown in the legend. About 50-100 resonant objects are needed to strongly distinguish ages that differ by only half a billion years.